中國機械工程學刊第四十二卷第六期第561~569頁(民國一百一十年)
Journal of the Chinese Society of Mechanical Engineers, Vol.42, No.6, pp. 561~569 (2021)

Investigation of Modal Characteristics and Milling Dynamics for a Machine-Tool System

Shen-Yung Lin *and Meng-Ru Song **

.

Keywords：Modal characteristics, Dynamic stiffness, Cutting stability, Spectrum analysis

ABSTRACT

The vibrations easily deduce the resonance or fatigue for a structure system and resulting in structure damage. Therefore, the modal characteristics of the structure itself should be investigated in detail, and make efforts to avoid the occurrence of resonance and unnecessary dissipation of loss. In addition to structure modal characteristics, process dynamics is another important factor that strongly related to cutting stability for machining accuracies of the machine-tool. An integrated execution methodology is proposed in this study for this purpose, in which the modal test, dynamic stiffness test and cutting experiments are performed step-by-step in a sequential manner. To this end, hammer, spectrum analyzer, accelerometer, ME'scope software and dynamometer are utilized together to conduct the tests and experiments on a CNC milling machine-tool, and the modal-related parameters and cutting process dynamics can systematically be investigated. From the synthesized results and investigations, it shows that the mode shapes, Mode 1 to Mode 3, mainly regarded to the deformation in head-stock and column structure components of a machine tool. While the main deformation parts corresponding to mode shapes of Mode 4 and Mode 5 are worktable and saddle, and these two modes exhibit a bending deformation behavior which will possibly make the joint interface to separate. The results from dynamic stiffness test show that when the head-stock moved along z-axis from -100mm height position down to -300mm location, the dynamic stiffness of the structure in x-axis direction may be changed from 217N/μm to 106N/μm, which have some impact on milling stability. The results from the milling experiment show that vibration marks left on the machined surface obviously under the conditions of cutting speed of 143.3m/min, feed rate of 400mm/ min and axial depth of cut of 0.5mm during up-milling process, and this phenomenon is judged as the chatter occurrence when comparing with those cases of stable milling state. The results obtained in this study can be utilized as a reference for milling parameter planning in industry.

Paper Received May, 2021. Revised June, 2021, Accepted June, 2021, Author for Correspondence: Shen-Yung Lin.

** Professor, Department of Mechanical and Computer-Aided Engineering, National Formosa University, Yunlin, Taiwan, ROC.*

*** Graduate Student Department of Mechanical and Computer-Aided Engineering, National Formosa University, Yunlin, Taiwan, ROC.*

INTRODUCTION

The machine-tool is the most basic equipment in the machinery manufacturing industry. Along with the development of the high-speed and precise machining technology, the requirement of dynamic performance of machine tools becomes higher and imperative. Among all various metal cutting techniques, milling is one of the most widely used cutting operation due to its flexibility in producing wide range of geometric shapes from deep pockets on the dies and molds to contours on aerospace parts. Machining accuracies are influenced both by the dynamic behavior of the machine-tool structure and the dynamics of the cutting process. The former may be analyzed using methods and theories related to structure modal characteristics. While process dynamics is less well understood, since theoretical and experimental methods for these studies are still under development.

Mahdavinejad (2005) used a finite element package software to modelling the instability of machining process dynamics of a turning machine system, in which the flexibility of machine-tool structure, workpiece and cutting-tool were accounted for. The natural frequencies and modal shapes are thus obtained from this dynamic model analysis which was corrected experimentally by modal testing on a turning machine. Furthermore, the stability lobes corresponding to response frequency of the developed model and modal analysis testing curves were also compared with each other. Thomas and Beauchamp (2003) conducted the dry turning experiments of mild carbon steels to investigate the effects of cutting variables on cutting force, cutting-tool vibration and the variations of cutting-tool modal parameters (natural frequency and damping). The cutting variables of cutting speed, feed rate, depth of cut, tool nose radius, tool length, workpiece length at different levels were taken into consideration. They designed a full factorial experiment and also accounted for the two-level and third-level interactions between and among the independent variables, respectively. Finally, the non-linear empirical models for predicting steady cutting forces and the variations in cutting-tool stiffness are thus developed as a function of the cutting parameters. Ahmadi and Ahmadian (2007) presented an approach in modeling machine-tool dynamics by using the measured dynamic flexibility of the holder-spindle assembly and an analytical model for the cutting-tool which is partly resting on a flexible support of this assembly. A zero thickness distributed elastic interface layer with variable stiffness was considered to represent the joint interface between the tool inserted shank portion and holder, i.e., the change in normal contact pressure along the inserted tool shank part is accounted for the tool-holder joint interface. A displacement-dependent energy dissipation mechanism in the joint interface is also involved in the model to account for the structurally damped characteristics of the joint interface. The experiments were conducted to verify the effectiveness of the proposed model and the efficiency in prediction of the cutting-tool dynamics in milling. Ertürk et al. (2007) developed an analytical model to investigate the effects of system design and operational parameters on the tool point frequency response function and hence on the chatter stability. The spindle geometry and bearing properties, and the properties of the holder and cutting-tool were considered as the design and operational parameters, respectively. Several useful conclusions have been drawn regarding the proper selection of the above parameters. Experimental verifications show that the model developed can be used to predict the stability lobe diagram which may be further modified in a predictable manner by selecting the favorable system parameters for maximizing the chatter-free material removal rate application. Iturrospe et al. (2007) proposed an approach to deal with the mode coupled system for orthogonal metal cutting process. The eigenvalues and eigenvectors of the coupled system obtained have been proven theoretically and experimentally and they are varied with the cutting conditions and structure modal parameters. The variations of system frequency and damping characteristic due to mode coupling have been employed for estimating the cutting-tool flank wear and cutting stability, respectively. Li and Liu (2008) proposed a chatter prediction model which can be applied in the simulation and analysis of milling dynamics on time domain. Several chatter detection criteria were also adopted to overcome the limitation which imposed by the single chatter criterion only. The instantaneous undeformed chip thickness was modeled to reflect the dynamic modulations by the cutting-tool vibrations while the regenerative effects are taken into consideration. The results of the stability lobes obtained from this numerical approach is consistent with those of analytical prediction verified by cutting tests. Su and Wang (2018) developed a force-excited vibration model to investigate the dynamic stiffness of a five-axis machine-tool during machining processes. The relationship between vibration displacement and dynamic stiffness can thus be constructed and used to illustrate the complex surface formation mechanism. The flank milling experiments using S shaped test piece were conducted as an example to examine the cutting behavior and machined surface qualities. Gupta et al. (2020) estimated the cutting-tool point dynamics through an output-only modal analysis with mass-change methods. An analytical model was also proposed to characterize the errors in eigenvector scaling and in natural frequency estimation systematically. The optimum size and location of the mass to be added on the cutting-tool may thus be guided by the model. The validated experiments both on a slender boring bar and an end mill show that the cutting-tool point frequency response functions have a good consistency and which were reconstructed regardless using modal parameters estimated by these proposed methods and using those obtained from the traditional EMA procedures. Hou et al. (2021) presented an approach of multiple damping and rigid supporters to improve the cutting stability in multi-axis milling of titanium hollow blade system. Firstly, a prediction model is developed to predict the dynamic parameters of blade machining system under a single damping supporter and rigid supporter. The effects of the supporter on the dynamic parameters and stability lobe curves are thus investigated. Then, the model is further applied in multipoint support system and the position optimization model is introduced simultaneously to determine the proper locations of multiple supporters. Finally, the effects of different supporting methods on the stability lobe diagrams and chatter suppression of blade system were analyzed and validated by blade machining experiments. It is shown that the optimized damping supporters can enhance the system stability more than optimized rigid supporters.

THEORETICAL FOUNDATION

Fast Fourier Transform

In the real signal measurement and analysis, the signal is measured in the time domain first and the Fourier transform is conducted for measured signal subsequently. The time domain is the initial presentation manner of the physical signal and it is also the most intuitively understandable presentation manner. However, the signal measured from the time domain may be transferred to the frequency domain through the fast Fourier transform, which not only highlights the periodic characteristics that were difficultly distinguished and explained in time domain but also can display the frequency components of the signal. The time domain signal is simple and direct while the frequency domain signal is easier to understand the physical meaning within it.

The vibration signals acquired in time domain sometimes cannot perfectly present the vibration-related information and the fast Fourier transform is often used in signal processing to convert the time domain signals into frequency spectrum. The basic theory is to assume that the record of the acquisition signal is an infinite and continuous periodic signal, and its fast Fourier transform (FFT) mathematical form is as follows:

$$F(\omega) = \int_{-\infty}^{\infty} f(t) \cdot e^{-j\omega t} dt \qquad (1)$$

$$f(t) = \frac{1}{2\pi} \int_{-\infty}^{\infty} F(\omega) \cdot e^{j\omega t} d\omega \qquad (2)$$

Where f(t) represents the original time domain signal, t represents time and ω represents angular speed to related with frequency domain.

It can be seen from equation (1) that the time interval of Fourier transform is from -∞ to ∞, so different frequency signals appear at any time, and after conversion, they can appear on the spectrum at the same time. The physical characteristics are easily observed as a time domain signal f(t) is converted to a frequency domain signal F(ω), as shown in Figure 1 and Figure 2. However, the above two conversions belong to the overall conversion, and the spectrum can only be obtained from the time domain representation of the overall signal, or the time domain of the signal can be obtained from the frequency domain representation of the overall signal. In addition, after Fourier transform, the frequency domain signal F(ω) displays the amplitude and phase of the individual frequency components in the time domain signal f(t). It cannot display the change of each frequency component of the signal over time and thus lacks its time information.

Fig 1 signal exhibited in time domain

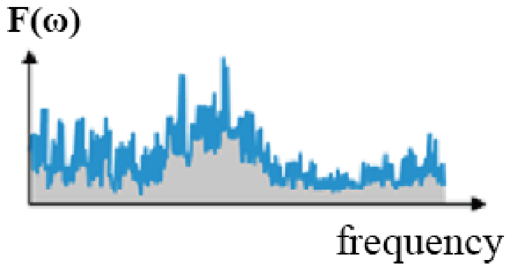

Fig 2 signal exhibited in frequency domain

Synchronous measurement of input (excitation) and output (response) operation is shown in Figure 3, the expression of input-output relationship in time domain is impulse response function and in frequency domain is frequency response function both are shown in Figures 4 and 5, respectively, and the frequency response function is obtained from the calculation of these two signals. Through the complex transformation of FFT, the amplitude magnitude and phase angle relationship can be known. In the fast Fourier transformation analysis, the system is assumed to be a linear system. that is, the functions obtained in time and frequency domains are additive and homogeneous. The auto-spectrum and cross-spectrum of the input and output are measured by a dual-channel FFT analysis technology to calculate coherence.

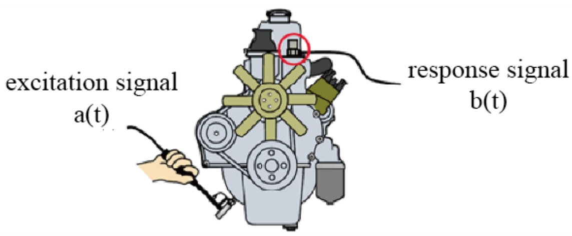

Fig 3 schematic diagram for synchronous measurement of excitation and response operation

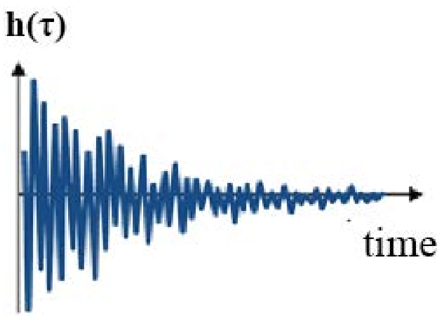

Fig 4 impulse response function

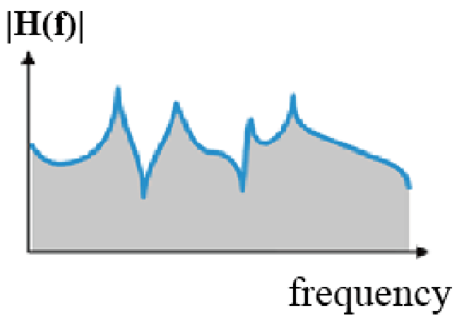

Fig 5 frequency Response function

Coherence Function

The coherence is used to examine the expression of the linearity between the input and output signals. Its related formula is as follows:

(a) Input-Output relationship

$$|G_{AB}(f)|^2 \leq |G_{AA}(f)| \cdot |G_{BB}(f)| \tag{3}$$

Where $G_{AB}(f)$ is the cross-correlation power, $G_{AA}(f)$ is the input auto-correlation power and $G_{BB}(f)$ is the output auto-correlation power.

(b) Definition of coherence function

$$\gamma^2(f) \equiv \frac{|G_{AB}(f)|^2}{|G_{AA}(f)| \cdot |G_{BB}(f)|} \tag{4}$$

It expresses degree of linear relationship between A(f) and B(f) and its range value is as follows:

$$0 \leq \gamma^2(f) \leq 1$$

Frequency Response Function

Figure 6 shows a typical single-input and single-output system. The time-domain input waveform is the impact force f(t), and the time-domain output waveform by the system is x(t). The frequency domain signals obtained by Fourier transform for the input and output time-domain waveforms is represented by F(ω) and X(ω), respectively.

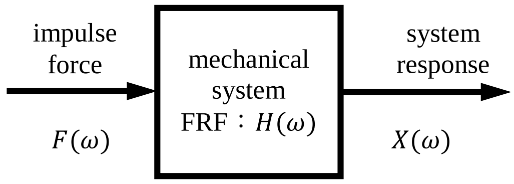

Fig 6 a typical single-input and single-output system

The frequency response function H(ω) can be defined as the ratio of the system output X(ω) to the system input F(ω) under harmonic excitation. It can also be called the transfer function. The common expression is as follows:

$$H(\omega) = \frac{Output}{Input} = \frac{X(\omega)}{F(\omega)} \tag{5}$$

The single degree of freedom (SDOF) system is shown in Figure 7. This system contains viscous damping, f(t) is the external force applied at the mass m, c is the damping coefficient, and k is the spring constant.

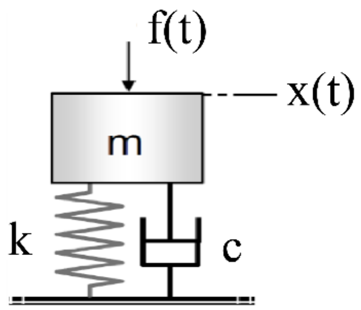

Figure 7 schematic diagram of a SDOF system

The governing equation of the system on time domain as follows:

$$ma = \mathrm{f} - cv - kx \leftrightarrow m\ddot{x} + c\dot{x} + kx = \mathrm{f} \tag{6}$$

Equation (6) through Laplace transform may be expressed as:

$$F = (mS^2X - v_0S - d_0) + (cSX - d_0) + kX \tag{7}$$

If the v_0 and d_0 terms in Equation (7) may be ignored, then the simplified frequency response function is:

$$\frac{X}{F} = \frac{1}{mS^2 + cS + k} \tag{8}$$

The frequency response function is a characteristic of a linear dynamic system and it will not change with the type of the input excitation function. The excitation function can be a sine function, a random function or a transient function in the time domain. The test results obtained by any kind of the excitation can be used to judge the response of the system by the excitation. Using the impulse excitation generated by the hammer is the simplest and fastest technique to obtain accurate structure frequency response function. However, impulse technology has a very high ratio of peak level to total energy, so it is not suitable for exploring the structural rigidity of the non-linear damping caused by the assembly tolerance, tightness or mechanical joints between structural components.

The overall structure of the machine tool is composed of large castings and related components, so it can be regarded as a multi-degree-of-freedom system composed of several masses m, spring k, and damping c. Assuming that an external force $f_n(t)$ is applied to the mass block, the system will generate a single degree of freedom displacement $x_n(t)$. The frequency response function diagram will show multiple natural frequency, damping ratio and dynamic stiffness values. These values will be presented in diagrams such as amplitude versus frequency, real part versus frequency, and imaginary part versus frequency. Each frequency response function diagram needs to cooperate with the appropriate judgmental method to find the natural frequency of the multi-degree-of-freedom system structure. The amplitude diagram is judged by the peak value of the wave, as shown in Figure 8(a); the real part graph meets Re=0 corresponding to the frequency position as refer to Figure 8(b); the imaginary part graph is the frequency corresponding to the extreme value as the natural frequency value as refer to Figure 8(c).

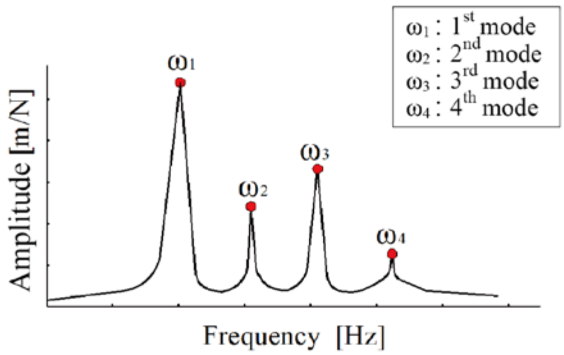

(a) amplitude versus frequency

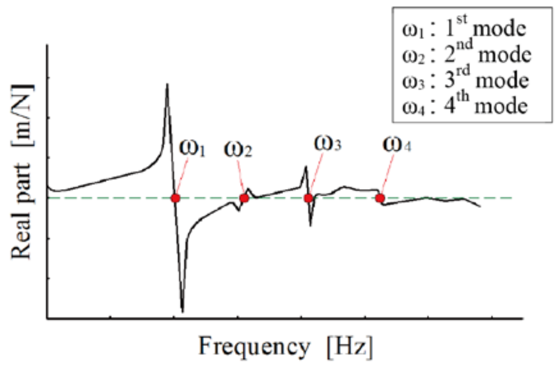

(b) real part versus frequency

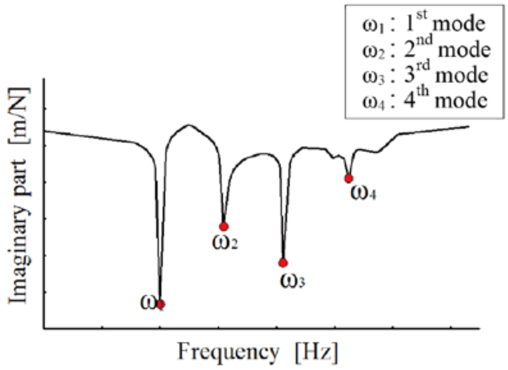

(c) imaginary part versus frequency

Fig 8 schematic diagram of frequency response function

EXPERIMENT

Modal Test

Experimental modal analysis is built on the system input/output data which they are already known. Through the use of this complete information regarding excitation (input) and response (output), the system parameter may be analyzed and identified. Structure modal test is carried out at a static manner under a manual excitation by human via the measurement of the excitation and response on two distinct locations. A dual-channel fast Fourier transform (FFT) analysis is performed subsequently to obtain the mechanical mobility function (transfer function) between any two points of the system. Through the curve fitting analysis of the mobility function by the modal analysis theory, the modal parameters of the available structures can be obtained and the mode shapes of the structure can be further established.

In this test, accelerometer is adhered on the structure and the hammer is used to offer an impact signal on the structure, the vibration energy through the transmission in the structure and being acquired by the detector of accelerometer. Through this experimental procedure the natural frequency of a machine-tool structure and its corresponding modal characteristics can thus be obtained. Schematic diagram for modal test of a CNC machine-tool is shown in Fig 9. Usually, a CNC milling machine-tool structure may be divided into five major parts, i.e. head-stock, column, base, saddle and worktable. There are 11, 14, 11, 10 and 13 response points arranged and distributed in head-stock, column, base, saddle, worktable parts, respectively. Totally, 59 response points in this machine-tool structure are constituted. Response measurement on these response points for each part in modal tests were shown in Fig 10.

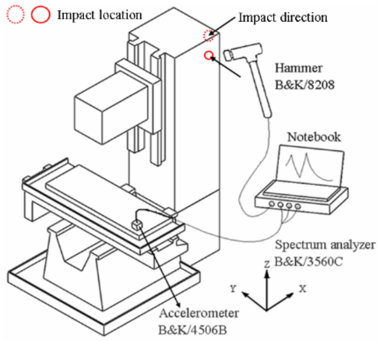

Fig 9 Schematic diagram for modal test of a CNC machine-tool

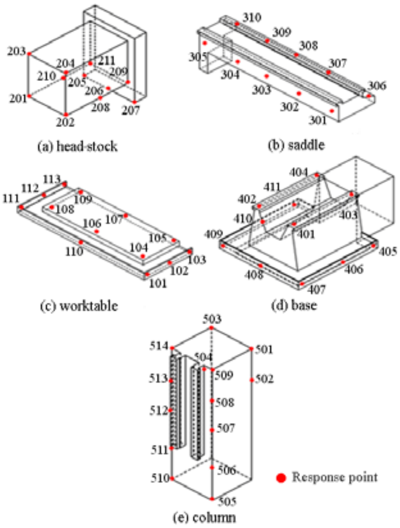

Fig 10 Response measurement positions for each part in modal tests

This test is done by a fixed impact point and then being excited consecutively on each response point through the application of the single input/single output method, and the frequency response function (FRF) on each response point is obtained every time. All the data of the FRF measurements would be collected and input into a modal analysis software called ME'scope and the modal analysis was performed accordingly. The purpose of this procedure is to determine the characteristic parameters related to structure mode and mode shape.

Dynamic Stiffness Test

In this study, dynamic stiffness test are conducted for a CNC machine-tool structure so as to investigate the variations of dynamic stiffness at different height positions of the head-stock. This test was conducted with 5 height positions of the head-stock along z-axis and 2 impact locations on a face-milling cutter, 10 combinations of test parameters totally are constituted for dynamic stiffness tests as shown in Table 1. While experimental set up for dynamic stiffness test is shown in Fig 11.

Table 1 Experimental planning for dynamic stiffness test

impact location	face-milling cutter along radial directions
Height position of the head-stock along z-axis (mm)	-100, -150, -200,- 250, -300

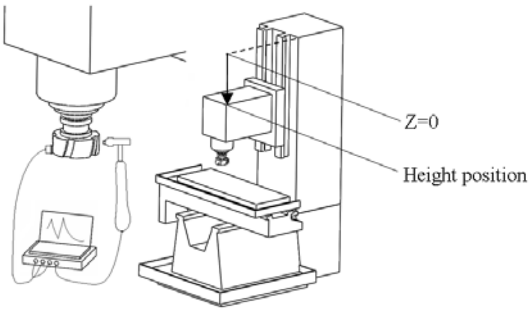

Fig 11 Experimental set up for dynamic stiffness test of a machine-tool

Milling Experiment

Aluminum alloy 6061-T6 was used as a workpiece in this study and two different milling manners, down-milling and up-milling are conducted in conjunction with different face-milling parameters. Table 2 shows the process parameters planning for face-milling experiment, i.e. 3 cutting speeds, 3 feed rates, 2 axial depth of cut and 1 radial depth of cut. Therefore, 36 combinations of cutting conditions totally were constituted for milling experiments. Milling experimental set up is shown in Fig 12. Here, cutting force and cutting tool vibration were monitored and measured by dynamometer and accelerometer, respectively during each milling process.

Table 2 Process parameters planning for face-milling experiment

Cutting speed, V(m/min)	143.3, 254.34, 367.38
Feed rate, F(mm/min)	200, 400, 600
Axial depth of cut, a_p(mm)	0.5, 1
Radial depth of cut, a_e(mm)	60

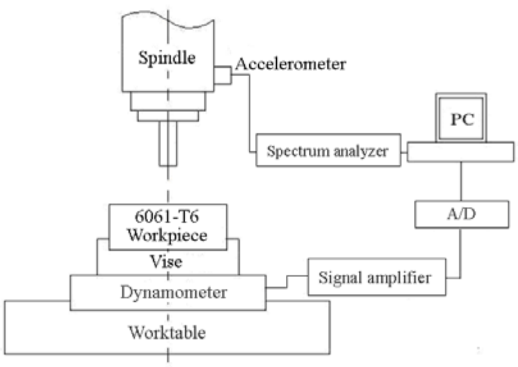

Fig 12: Milling experiment set up

RESULTS AND DISCUSSION

Modal Characteristics

As mentioned above, all the data related to FRF measurements at the response points are collected together and input into a modal analysis software. Fig 13 shows the collections of all the modal frequency response functions from experimental modal analysis (EMA). The collection consists of real part, imaginary part and phase angle of the FRF. Fig 14 shows the curve-fitting of all these FRF, which exhibits the modal peak function by using imaginary part of the FRF. These modal peaks clearly represent the possible resonant frequency detected for a CNC milling machine-tool structure. The natural frequency and the corresponding mode shape, and modal characteristic parameter for this structure object are shown in Table 3 Here, MAC represents the modal assurance criterion for mode shape and its value ranges between 0 and 1. If MAC close to 1, the mode shapes synthesized from all the components strongly depends on the real data and it is highly reliable. Conversely, if MAC far from 1, the mode shapes do not depends on the real data and low reliability is accompanied.

The mode shapes shown in Table 3 show that Mode 1 to Mode 3 mainly related to the deformation in head-stock and column parts of the machine-tool structure. While the main deformation parts corresponding to mode shapes of Mode 4 and Mode 5 are worktable and saddle and these two modes exhibit bending deformation behavior will possibly make the joint interface to separate.

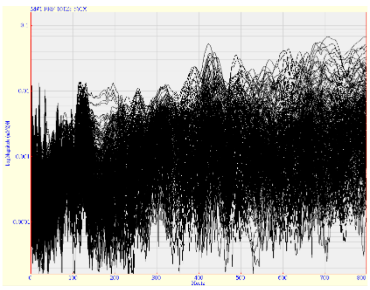

Fig 13 Collections of all the modal frequency response functions from EMA

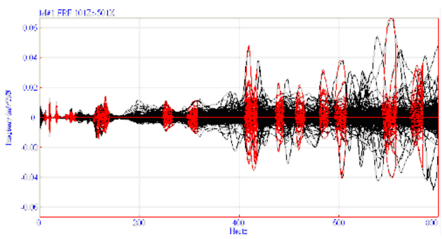

(a)

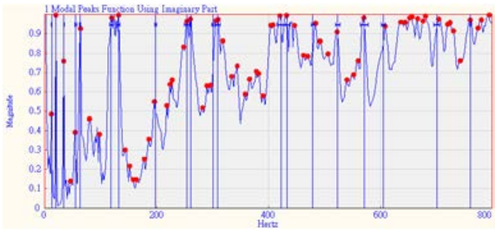

(b)

Fig 14 Curve-fitting chart. (a) imaginary part of the FRF; (b) modal peak function using imaginary part

Table 3 Modal parameters and mode shape for 1st to 5th mode of a machine-tool

mode	Frequency (Hz)	mode shape	damping	damping ratio (%)	MAC
1	12.63	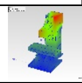	0.4154	3.287	0.9355
2	19.98	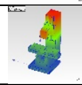	0.397	1.987	0.9775
3	34.41	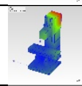	0.7426	2.158	0.9562
4	55.35	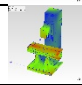	1.677	3.029	0.6677
5	63.09	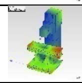	1.321	2.093	0.6255

Dynamic Stiffness

Fig 15 shows the comparisons of dynamic stiffness along different axial directions for a machine-tool structure at different height positions of head-stock. It can be observed that the dynamic stiffness along y and z axial directions is not varied obviously at different height positions. The cutting performance affected by the dynamic stiffness along these two axial directions is greatly reduced. While dynamic stiffness along x-direction is varied obviously at different height positions of head-stock. Note that, dynamic stiffness is varied from 217 to 106 N/μm when the head-stock moves from -100mm position down to -300mm locations, which will have some impact on milling stability. Therefore, this dynamics may have a greater chance on the effect of cutting performance.

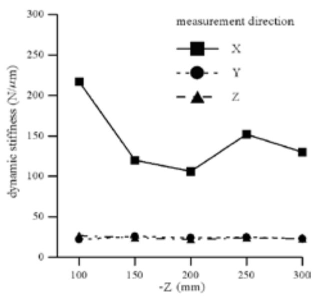

Fig 15 Comparisons of dynamic stiffness along different axial directions for a machine-tool structure

at different height positions of head-stock

Cutting Stability

Fig 16 and Fig 17 show the relationship between tangential cutting force component and feed rate at different cutting speed under axial depth of cut of 0.5mm in down-milling. Averagely, this cutting force component in down-milling is greater than those in up-milling. The chip thickness is varied from bigger to smaller during the down-milling process. The cutting tool-edge has an impact contact with the workpiece at the initial engagement stage, larger contact area results in a greater cutting force consequently. While in the up-milling situation the chip thickness is varied from smaller to bigger in contrast to down-milling, so the impact force will be relatively small during the milling process. Observations on the machined surface, vibration marks left on the machined surface obviously under the conditions of cutting speed of 143.3 m/min, feed rate of 400 mm/ min and axial depth of cut of 0.5 mm during up-milling process as shown in Fig 18, this phenomenon is judged as the chatter occurrence when comparing with those cases of stable milling operation as shown in Fig 19 Cross comparisons between cutting forces and machined surface patterns, stable cutting forces according with good surface quality are found under the cutting speed of 254.34m/min regardless of which feed rates and axial depths of cut set. This cutting condition can be used as a basis for future machining application. Also, these results can be utilized as a reference for milling parameter planning in industry.

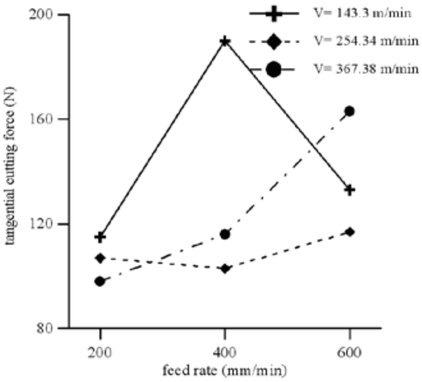

Fig 16 Relationship between tangential cutting force component and feed rate at different cutting speed under 0.5mm axial depth of cut in down-milling

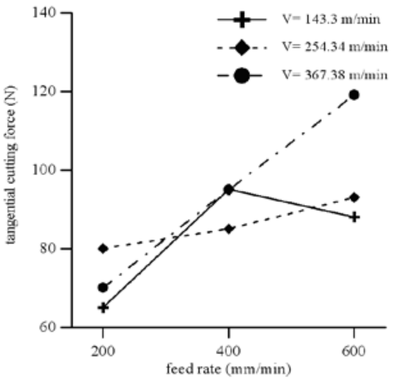

Fig 17 Relationship between tangential cutting force component and feed rate at different cutting speed under axial depth of cut of 0.5mm in up-milling

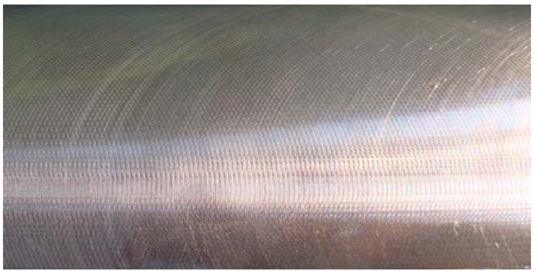

Fig 18 Surface pattern under the conditions of cutting speed of 143.3m/min, feed rate of 400mm/min and axial depth of cut of 0.5mm

Fig 19 Surface pattern under the conditions of cutting speed of 254.34m/min, feed rate of 200mm/min and axial depth of cut of 1mm

CONCLUSION

In order to investigate the modal characteristics and its cutting dynamics during milling process for the machine-tool, an integrated execution methodology is proposed in this study for this request. In which, the modal test, dynamic stiffness test and cutting experiments are performed step-by-step in a sequential manner. The modal parameters and cutting performance are thus obtained systematically. From the above analyses, the following conclusions can be drawn.

1. The maximum spindle speed is 6000rpm for this CNC milling machine-tool, the highest frequency induced is 100Hz. From the results of modal test, Mode 1 to Mode 5 falls within this frequency range and they will possibly lead to a resonance.

Mode 1 to Mode 3, mainly relates to the deformation in head-stock and column structure parts of the machine-tool. While the main deformation parts corresponding to mode shape, Mode 4 and Mode 5, are worktable and saddle parts and these two modes exhibit bending deformation behavior will possibly make the joint interface to separate. Thus, strengthening stiffness in worktable and saddle joints will help to improve the cutting ability.

2. The dynamic stiffness along x-axis is varied from 217 to 106 N/μm when the head-stock moves from -100mm position down to -300mm location. The cutting performance will be affected due to this dynamic change. While the dynamic stiffness along the other two directions, y and z axes, play a minor role on the effect of cutting performance.

3. It is found that there is chatter occurred under the conditions of cutting speed of 143.3m/min, feed rate of 400mm/min and axial depth of cut of 0.5mm. It has to avoid this process parameter combination setting for practical use.

4. Cross comparisons between cutting forces and machined surface patterns, stable cutting forces according with good surface quality are found under the cutting speed of 254.34m/min regardless of which feed rates and axial depths of cut set. It can be used as a basis for future machining application.

REFERENCE

Ahmadi, K. and H. Ahmadian, "Modelling machine tool dynamics using a distributed parameter tool-holder joint interface", *International Journal of Machine Tools and Manufacture,* Vol.47, pp.1916-1928 (2007)

Ertürk, A., E. Budak and H. N. Özgüven, "Selection of design and operational parameters in spindle-holder-tool assemblies for maximum chatter stability by using a new analytical model", *International Journal of Machine Tools and Manufacture*, Vol.47, pp.1401-1409 (2007)

Gupta, P., M. Law, and S. Mukhopadhyay, "Evaluating tool point dynamics using output-only modal analysis with mass-change methods", *CIRP Journal of Manufacturing Science and Technology*, Vol.31, pp.251-264 (2020)

Hou, J., Z. Zhao, Y. Fu, and N. Qian, "Machining stability enhancement in multi-axis milling of titanium hollow blade by introducing multiple damping and rigid supporters," *Journal of Manufacturing Processes*, Vol.64, pp.198-208 (2021)

Iturrospe, A., V. Atxa and J. M. Abete, "State-space analysis of mode-coupling in orthogonal metal cutting under wave regeneration", *International Journal of Machine Tools and Manufacture,* Vol.47, pp.1583-1592. (2007)

Li, Z. and Q. Liu, "Solution and analysis of chatter stability for end milling in the time-domain", *Chinese Journal of Aeronautics*, Vol.21, pp.169-178 (2008)

Mahdavinejad, R., "Finite element analysis of machine and workpiece instability in turning", *International Journal of Machine Tools and Manufacture.* Vol.45, pp.753-760 (2005)

Su, Z. and L. Wang, "Effect of the dynamic characteristics of a five-axis machine tool on the surface quality of complex surface", *Procedia CIRP*, Vol.72, pp.1505-1511 (2018)

Thomas, M. and Y. Beauchamp, "Statistical investigation of modal parameters of cutting tools in dry turning", *International Journal of Machine Tools and Manufacture,* Vol.43, pp.1093-1106 (2003)

工具機結構模態特性與銑削動態之研究

林盛勇　　宋孟儒

國立虎尾科技大學機械與電腦輔助工程系

摘 要

振動易造成結構的共振或疲勞從而破壞結構，因此必須詳細研究結構本身的模態特性，盡力去避免共振的發生以及不必要的損失消耗。切削製程動態是另外一個影響切削穩定性的重要因子，它與切削穩定性強烈相關，關係到工具機加工的精度。為此，本文提出一整合性的執行方法，以逐步依序之方式進行模態測試、動剛性測試及銑削實驗。藉由結合使用敲擊錘、頻譜分析儀、加速規、ME'scope軟體及動力計，在一銑床上完成上述之測試與實驗，模態相關參數與切削過程動態則能夠有系統地被檢視。綜合以上之結果與探討顯示，Mode 1至Mode 3其模態振型影響之結構部件為頭座與立柱。而Mode 4及Mode 5所對應的模態振型，主要變形部件為工作台與鞍座，這兩個模態的彎曲變形將造成接合面可能的分離。動剛性實驗結果顯示，當頭座沿Z軸高度從-100mm降至-300mm時，X軸向結構動剛性從217 N/μm變化至106 N/μm，對切削穩定性將有所影響。銑削實驗結果顯示，逆銑過程當切削速度143.3 m/min、進給率400 mm/min及切削深度0.5 mm時，加工表面出現顫紋，與穩定切削之結果比對研判該銑削條件組合已發生切削顫振。以上這些結果可作為日後銑削製程參數規劃之參考。